Applied Surface Science xxx (2013) xxx–xxx

Contents lists available at ScienceDirect

Applied Surface Science

journal homepage: www.elsevier.com/locate/apsusc

Preparation and characterization of multilayer NiO nano-products via electrospinning

Mengzhu Liu [a], Yongpeng Wang [a], Pengchong Li [b], Zhiqiang Cheng [a,c], Yongqiang Zhang [a], Mingyue Zhang [a], Meijuan Hu [a], Junfeng Li [a,*]

[a] College of Chemistry, Jilin University, Changchun 130012, People's Republic of China
[b] College of Electronic Science and Engineering, Jilin University, Changchun 130012, People's Republic of China
[c] College of Resources and Environment, Jilin Agriculture University, Changchun 130118, People's Republic of China

ARTICLE INFO

Article history:
Received 7 April 2013
Received in revised form 19 July 2013
Accepted 22 July 2013
Available online xxx

Keywords:
Electrospinning
Multilayer
Nanofibers
Nanogrooves
Formaldehyde
Sensor

ABSTRACT

NiO with multilayer structure was prepared by impregnating electrospun polylactic acid (PLA) nanofibrous webs with nickel acetate solution and subsequent calcination. From SEM images, it can be observed that the structures of NiO products from surface to center were nanogrooves inlaid film, hollow pores and honeycomb-like nanofibers with nanogrooves, successively. The formation mechanisms were studied in detail by TGA and DSC. FT-IR and XRD measurements demonstrated that the product was highly pure NiO with cubic structure. The sensitivity of the NiO products to formaldehyde was investigated. As a result, the multilayer NiO exhibited much higher sensing signal than NiO powders. This indicated that the prepared multilayer NiO could be used as a candidate to fabricate formaldehyde sensors.

1. Introduction

Nickel oxide (NiO) is an attractive material because its physical properties are important for many promising applications in the field of catalyst [1], battery electrode [2], electrochromic devices [3], antiferromagnetic material [4] and chemical sensors [5]. It is well known that material properties are strongly dependant on its structure [6]. Thus, making changes on structure of nanomaterials is promising to obtain specific property and realize specific application. In recent years, there have been many efforts in the fabrication of nanostructure NiO with various morphologies to improve its performance [7–11]. Among these morphologies, it has been found that the structure with high specific surface area can exhibit much more excellent performance in catalyst and gas sensor [12,13]. In order to obtain nanostructure with properties of high surface area-to-volume and length-to-diameter ratios, electrospinning is employed [14]. It is a versatile and mature method [15] that can produce polymer fibers in diameter ranging from micrometers to nanometers. However, via electrospinning, NiO have been only fabricated in types of nanotubes [16] and nanofibers [17] up to now. To further exploit its applications, new special structures are required.

Formaldehyde is a volatile organic compound which is considered as one of the most important indoor air pollutants. It could cause health problems such as bronchial asthma, atopic dermatitis, sick building syndrome and even leukemia. According to these serious consequences, a high sensitive sensor is needed. NiO has been studied as a sensing layer for formaldehyde detection recently. Dirksen et al. [18] have reported the suitability of pure and doped NiO as a thin film resistive gas sensor for formaldehyde. Lee et al. [19] have successfully demonstrated a novel self-heating formaldehyde gas sensor based on a thin NiO sensing layer. Castro-Hurtado et al. [20] have studied the influence of structural properties and thickness of NiO thin films on formaldehyde detection. It can be discovered that NiO thin films sensors are usually used, whereas NiO with special structures are rarely employed.

In this study, a new multilayer NiO which is expected to have applications in gas sensors was prepared by impregnating electrospun polyactic acid (PLA) nanofibrous webs with nickel acetate solution and subsequent calcination. The calcined samples were elucidated by TGA, DSC, FT-IR, XRD and SEM respectively and the formation mechanisms of the different structures were investigated. In addition, comparison of the sensitivity to formaldehyde between multilayer NiO and NiO powders was carried out.

* Corresponding author. Tel.: +86 0431 85164704.
E-mail addresses: liumengzhu125@163.com (M. Liu), wyp4889@gmail.com (Y. Wang), chongpengli@sina.com (P. Li), czq5974@163.com (Z. Cheng), zhang_yongqiang85@163.com (Y. Zhang), zhangmingyue8803@163.com (M. Zhang), 442675083@qq.com (M. Hu), jfli@jlu.edu.cn (J. Li).

0169-4332/$ – see front matter © 2013 Elsevier B.V. All rights reserved.
http://dx.doi.org/10.1016/j.apsusc.2013.07.118

2. Experimental

2.1. Materials

Nickel (II) acetate tetrahydrate ($(CH_3COO)_2Ni{\cdot}4H_2O$) was purchased from Tianjin Huadong Chemical Regents, China. Polylactic acid (PLA, Mw = 300,000 g/mol) was obtained from Shandong Institute of Medical Equipment. 1,1,1,3,3,3-Hexafluoro-2-propanol (HFIP, Aladdin Reagent, Shanghai, China) and ethanol (Beijing Chemical Works, China) were used as solvents directly. All other chemicals (analytical grade reagents) were purchased from Tianjin Chemicals Co. Ltd. (Tianjin, China), and used as received.

2.2. Preparation of NiO products

The electrospinning solution was prepared by dissolving PLA in HFIP at a concentration of 8 wt.%. After vigorously stirring for 4 h, a transparent solution for electrospinning could be obtained. The polymer solution was loaded into a glass dropper which was connected to a high-voltage supply (DW-P303-5AC High Voltage (0–30 kV), Dongwen High-voltage Power-supply Company, China). The voltage for electrospinning was 15 kV. A piece of flat aluminum foil was used to collect the nanofibers. The distance between the tip of the dropper and the collector was 20 cm. All electrospinning process was carried out at ambient temperature. The fibers were exposed to air overnight for stabilization, and then were impregnated with 6 wt.% ethanol solution of nickel acetate for 2 days. After drying, the sample was calcined at 600 °C for 4 h in air. NiO powder was prepared by calcinating the pure $(CH_3COO)_2Ni{\cdot}4H_2O$ powders at the same condition.

2.3. Characterization

Thermal gravimetric analysis (TGA) was carried out by using PerkinElmer Pyris 1 TGA (United States) from room temperature to 700 °C at a heating rate of 10 °C/min under a flowing air atmosphere. Differential scanning calorimeter (DSC) measurements were performed on a Mettler Toledo DSC821^e instrument (Switzerland) at a heating rate of 20 °C/min from room temperature to 400 °C under nitrogen. Fourier transform-infrared radiation (FT-IR) spectrometer (SHIMDZU, 1.50SU1, Japan) was used to identify the vibration in functional groups presented in the fibers. The phase structures of the calcined nanofibers were identified by X-ray diffraction (XRD), which was performed on a Siemens D5005XRD diffractometer. The morphology and dimensions of the fibers were analyzed by scanning electron microscope (SEM) (SHIMDZU SSX-550, Japan).

2.4. Testing of sensors

The as-calcined sample was mixed with deionized water in a weight ratio of 100:20 to form a paste. The paste was coated on a ceramic tube on which a pair of gold electrodes was previously printed, and then a small Ni–Cr alloy wire was placed through the tube as a heater, which provided operating temperature for the sensors. The thickness of the sensing films was measured to be about 300 μm. Gas sensing properties were measured using a static test system [21]. Saturated target vapor was injected into a test chamber (20 L in volume) by a micro-injector through a rubber plug. After fully mixed with air (relative humidity was about 25%), the sensor was put into the test chamber. When the response reached a constant value, the sensor was taken out to recover in air. The electrical properties of the sensor were measured by a CGS-8 (Chemical Gas Sensing) intelligent analyze system [22]. Sensing measurement was purchased from Beijing Elite Tech Co. Ltd. (Beijing, China).

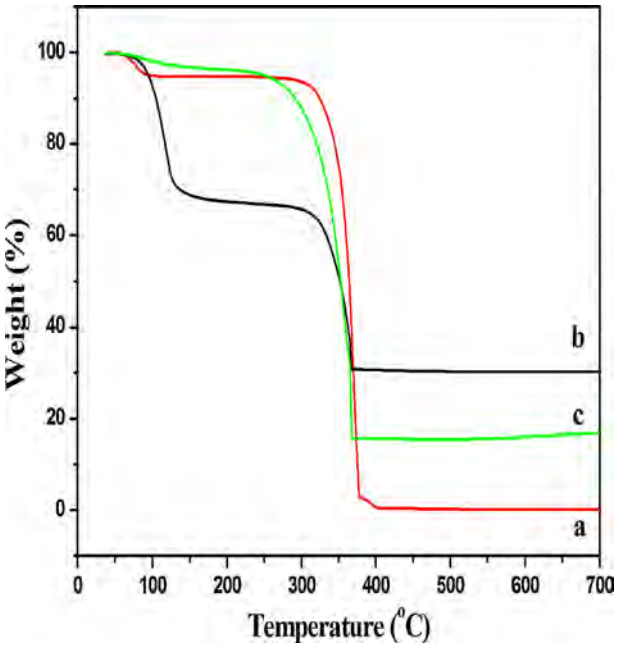

Fig. 1. TGA curve of (a) pure PLA nanofibers, (b) pure $(CH_3COO)_2Ni{\cdot}4H_2O$ powders, and (c) PLA/$(CH_3COO)_2Ni{\cdot}4H_2O$ composite nanofibers.

3. Results and discussion

3.1. Thermal analysis

Thermograms of pure PLA nanofibers, pure $(CH_3COO)_2Ni{\cdot}4H_2O$ powders and PLA/$(CH_3COO)_2Ni{\cdot}4H_2O$ composite nanofibers were shown in Figs. 1 and 2. As shown in Fig. 1(a), the pure PLA nanofibers presented a weight loss between 50 °C and 90 °C. This was ascribed to the loss of moisture and trapped solvent (water and HFIP). From 309 °C to 400 °C, another weight loss was observed. This was corresponding to the decomposition of PLA. After 400 °C, no more weight loss can be seen, indicating the PLA was decomposed

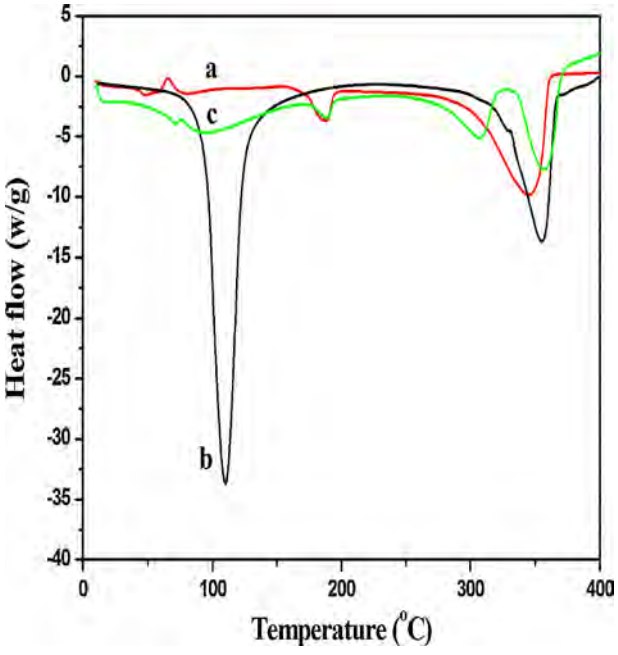

Fig. 2. DSC curve of (a) pure PLA nanofibers, (b) pure $(CH_3COO)_2Ni{\cdot}4H_2O$ powders, and (c) PLA/$(CH_3COO)_2Ni{\cdot}4H_2O$ composite nanofibers.

Please cite this article in press as: M. Liu, et al., Preparation and characterization of multilayer NiO nano-products via electrospinning, Appl. Surf. Sci. (2013), http://dx.doi.org/10.1016/j.apsusc.2013.07.118

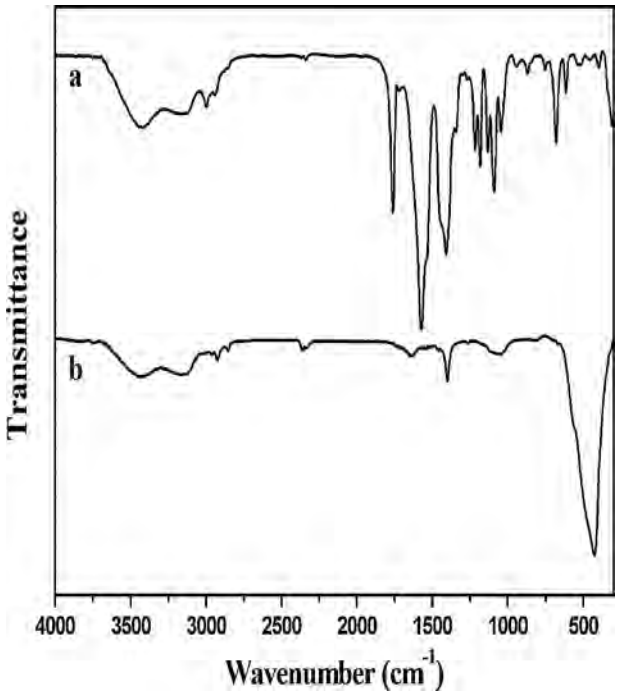

Fig. 3. FT-IR spectra of PLA/$(CH_3COO)_2Ni{\cdot}4H_2O$ composite nanofibers (a) before and (b) after calcination.

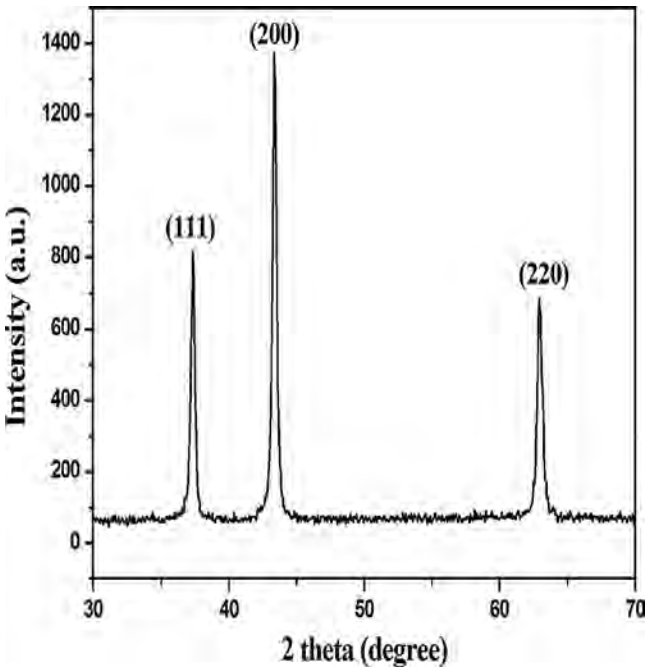

Fig. 4. XRD pattern of PLA/(CH3COO)$_2$ Ni·$4H_2O$ composite nanofibers after calcination.

completely. The TGA curve of pure $(CH_3COO)_2Ni{\cdot}4H_2O$ powders (Fig. 1(b)) seemed to exhibit two stages of decomposition: the first stage appeared from 82 to 120 °C was attributed to part decomposition of $(CH_3COO)_2Ni{\cdot}4H_2O$ and liberation of the crystal water; the second stage occurred in the range of 300–370 °C was related with the complete decomposition of $(CH_3COO)_2Ni$. The TGA curve of PLA/$(CH_3COO)_2Ni{\cdot}4H_2O$ blend was shown in Fig. 1(c). Referring to the analyses above, the slight weight loss (~6.2%) from room temperature to 256 °C corresponded to the loss of moisture. The dramatic weight loss (~84%) occurred at 256–367 °C was own to complete decomposition of PLA and $(CH_3COO)_2Ni$. The shift of the decomposition temperature of PLA should be due to the presence of nickel oxide in the samples. When the temperature reached about 400 °C, the curve became flat, demonstrating that the composite nanofibers had transformed into inorganic oxide completely.

DSC measurement was performed in a range of room temperature to 400 °C in order to provide further evidence for the presence of various species and evaluate their thermal behavior as shown in Fig. 2. The exothermic peaks at 66 °C in Fig. 2(a) and 74 °C in Fig. 2(c) were corresponding to the glass transition temperature (Tg) of PLA. The sharp peak at 109 °C in Fig. 2(b) and the broad peak at about 95 °C in Fig. 2(c) were caused by the loss of moisture and the melt of $(CH_3COO)_2Ni$. The endothermic peaks occurred at 186 °C (Fig. 2(a) and (c)) were generated from the melt of PLA. The peaks at 344 °C in Fig. 2(a) and 306 °C in Fig. 2(c) were the decomposed peaks of PLA. The peaks at 355 °C in Fig. 2(b) and 357 °C in Fig. 2(c) belonged to the complete decomposition of $(CH_3COO)_2Ni$. The above analyses accorded with the TGA results well.

3.2. Structure inspections

Fig. 3 showed the FT-IR spectra of the PLA/$(CH_3COO)_2Ni{\cdot}4H_2O$ blended nanofibers before and after calcination. As shown in Fig. 3(a), the broad bands at 3438 and 3140 cm^{-1} were assigned to the O—H asymmetrical stretching vibration, which came from H_2O in $(CH_3COO)_2Ni{\cdot}4H_2O$. The band at 2999, 1765, 1570, 1406, 1190, 1094 and 684 cm^{-1} was attributed to the vibrations of C—H, C=O, C—O and C—C which existed in PLA and $(CH_3COO)_2Ni{\cdot}4H_2O$ [23,24]. After treating at 600 °C (Fig. 3(b)), the organic groups disappeared and a new peak came out. The peak existed at about 430 cm^{-1} was the stretching vibration of Ni—O [25]. This demonstrated once again that under the function of heat treatment, PLA was decomposed completely and NiO was produced. The weak transmission band at 1645 cm^{-1} was the H–O–H bending mode of molecularly absorbed water on the NiO. And the corresponding peak of the stretching vibration of H–O–H appeared at 3438 and 3140 cm^{-1}. This indicated NiO had a good property of hygroscopicity.

XRD patterns of the calcined samples were given in Fig. 4. Well-defined diffraction peaks at about 37.2°, 43.3° and 62.9° were observed, corresponding to the (1 1 1), (2 0 0) and (2 2 0) planes of cubic NiO crystals [26], respectively. The XRD pattern confirmed that the product was well crystallized NiO with high purity.

3.3. Morphology and formation mechanism

Fig. 5(a) and (b) exhibited SEM images of PLA nanofibers and PLA/$(CH_3COO)_2Ni{\cdot}4H_2O$ composite nanofibers respectively. As shown in Fig. 5(a), the electrospun PLA nanofibers lay randomly with an average diameter of approximately 430 nm, resulting in a two-dimensional PLA nanofiber network. It was also evident that these PLA nanofibers crossed and overlapped with each other, forming lots of distinct junctions. At each of these junctions, the upper nanofiber was slightly suspended due to the presence of the lower one. After immersing in nickel acetate solution, PLA nanofibers were slightly modified (Fig. 5(b)). The outer layer was filled with nickel acetate, so that the junctions between the fibers cannot be observed clearly.

The SEM images of sintered products were shown in Fig. 6. Interestingly, the products exhibited multilayer structure after calcination (Fig. 6(a)). As shown in Fig. 6(b), the fibers in outer layer seemed to be inlaid in the surface and the junctions between these nanofibers seemed to be welded. The average diameter of nanogrooves on the surface was about 262 nm, which was much smaller than the one of pure PLA. The formation mechanism was shown in Fig. 7(a). At first, the outer layer fibers adsorbed large

Please cite this article in press as: M. Liu, et al., Preparation and characterization of multilayer NiO nano-products via electrospinning, Appl. Surf. Sci. (2013), http://dx.doi.org/10.1016/j.apsusc.2013.07.118

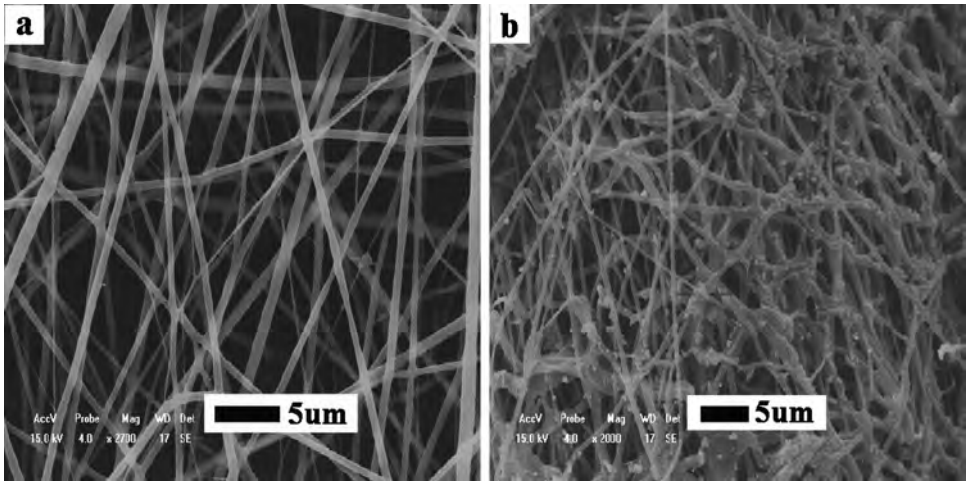

Fig. 5. SEM images of (a) pure PLA nanofibers, and (b) PLA fibers immersed in $(CH_3COO)_2$ Ni·$4H_2O$ solution for 2 days.

amounts of nickel acetate. Then in the following heat treatment, the nickel acetate crystallites melted before decomposition because of its low melting point. Thus, the nickel acetate formed an interconnected structure and encapsulated the PLA fibers. With the increase of temperature, PLA fibers melted and decomposed gradually. The generated gas can only be released from the surface where the nickel compound shell was thinnest. As a result, the morphology was formed.

Fig. 6(c) showed the cross section of the outer layer. It can be observed that the inlaid nanofibers were hollow. The average diameter of the pores was about 282 nm, which was close to the diameter of the nanogrooves on the surface. The possible mechanism was

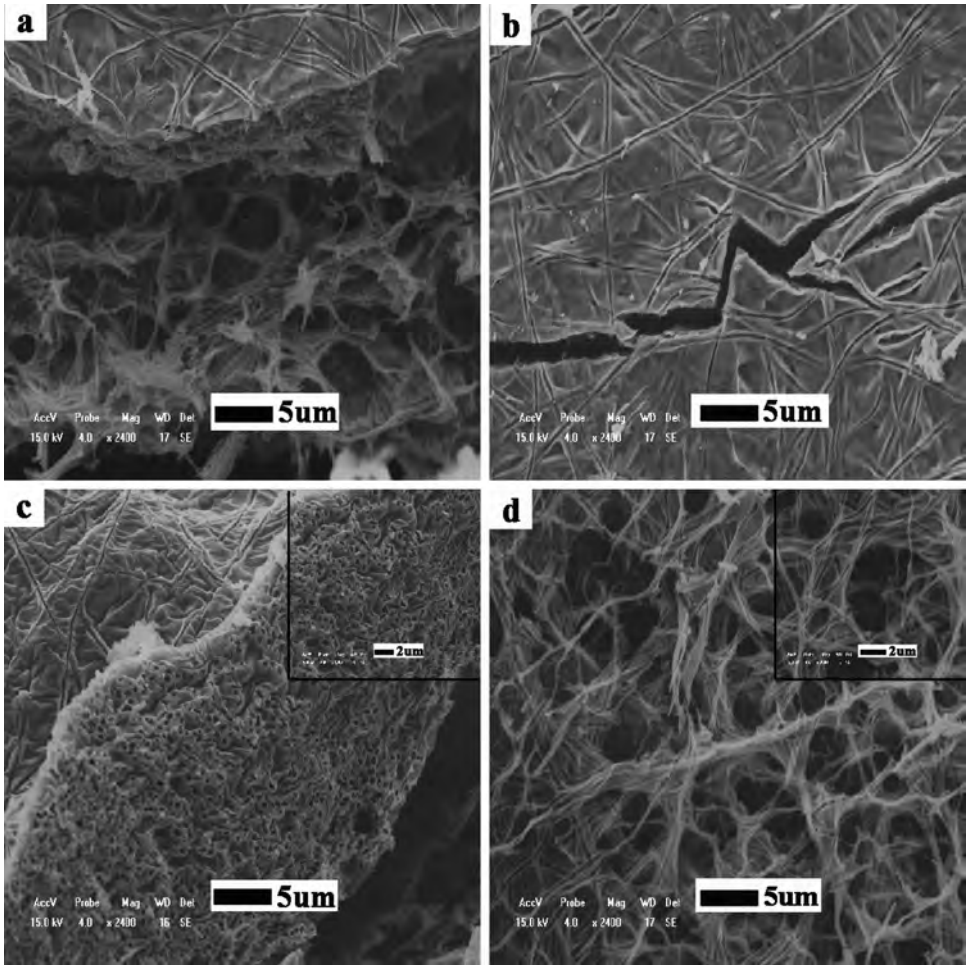

Fig. 6. SEM images of NiO products from different positions: (a) cross section of whole NiO film, (b) vertical view of the surface, (c) cross section of the surface, and (d) vertical view of the part under the surface. Inset images are the corresponding higher magnifications.

Please cite this article in press as: M. Liu, et al., Preparation and characterization of multilayer NiO nano-products via electrospinning, Appl. Surf. Sci. (2013), http://dx.doi.org/10.1016/j.apsusc.2013.07.118

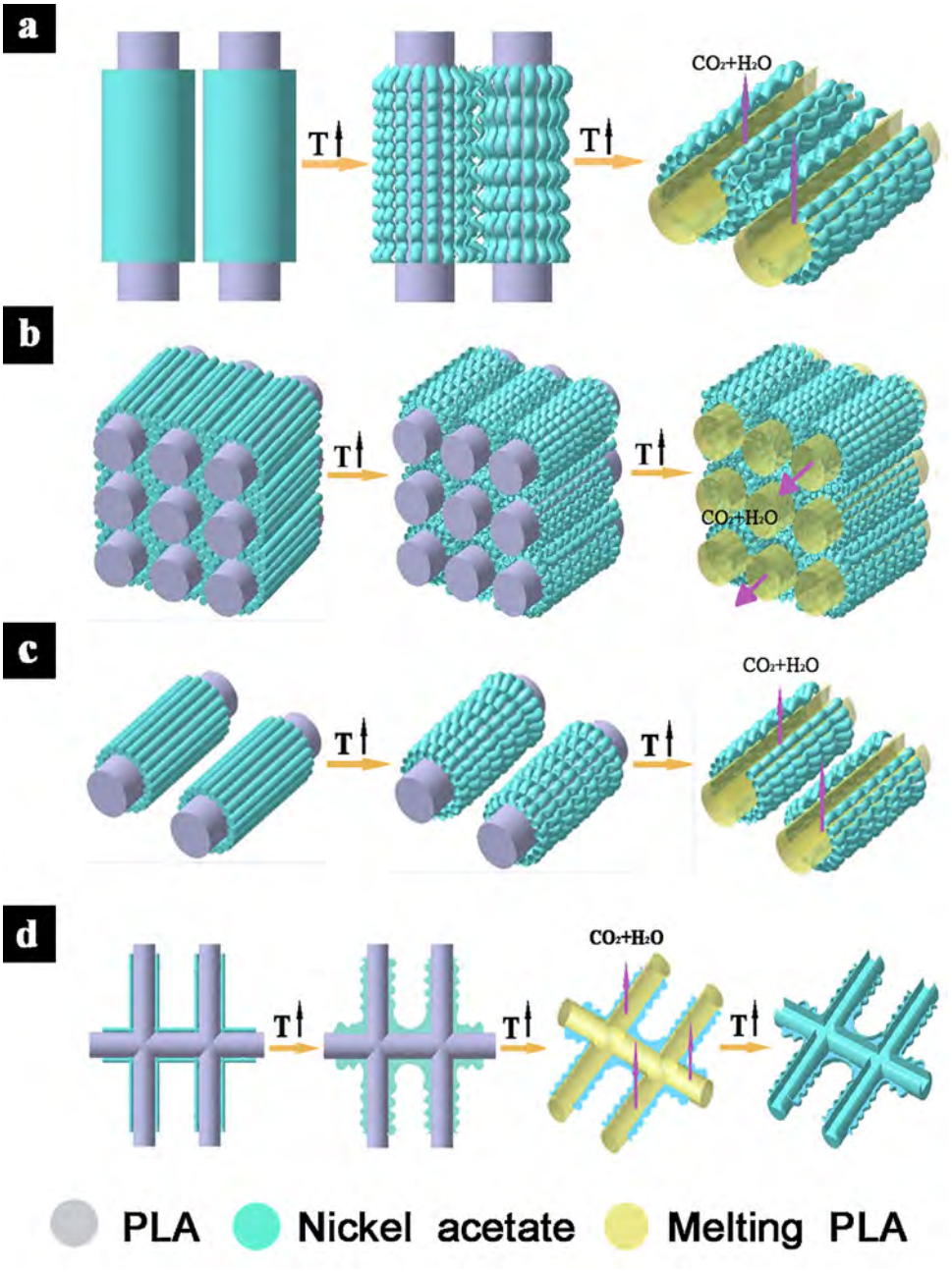

Fig. 7. Formation mechanism of (a) surface of the NiO film, (b) cross section of the surface, (c) the part under the surface, and (d) the circular pores and the nanogrooves.

shown in Fig. 7(b). It was a little different from the surface part. With the increase of the distance from surface, PLA fibers stacked randomly with nickel acetate surrounded. Each PLA fiber had a very thick nickel acetate shell, so the generated gas can only be released from the channel that provided by decomposition of PLA.

Under the surface where the amount of nickel acetate was less, the product presented a structure of honeycomb (Fig. 6(d)). In the honeycomb-like structure, many round pores with diameter in the range of 1.0–4.2 μm can be observed. The honeycomb-like structure was constituted by many continuous nanobelts, with nanogrooves of 125–300 nm in width on it. The appearance of the nanogrooves resulted in the increase of surface area. The formation of honeycomb-like structure had been reported by Qiu et al. [27]. The mechanism was shown in Fig. 7(c) and (d). In the less nickel acetate area, on one hand, PLA fibers were far from each other so that the melted nickel acetate cannot form a connected structure. On the other hand, PLA fibers had mechanical stability. The two points made the basic structure of the web preserve after heat treatment. What is more, driven by surface tension, the melted nickel acetate produced some round bulging at the corners of the interspaces between fibers, making the polygonal corners formed by linear PLA nanofibers become round. Thus, circular pores were formed. In this middle part of the film, PLA fibers were surrounded tightly by nickel acetate, and the decomposed gas cannot find a channel to release. As a result, the layer burst during heating, forming nanogrooves.

3.4. Sensing characteristics

Fig. 8 depicted the response values of sensors fabricated from NiO powders and NiO products to 100 ppm and 500 ppm formaldehyde at different temperatures. On one hand, the values increased

Please cite this article in press as: M. Liu, et al., Preparation and characterization of multilayer NiO nano-products via electrospinning, Appl. Surf. Sci. (2013), http://dx.doi.org/10.1016/j.apsusc.2013.07.118

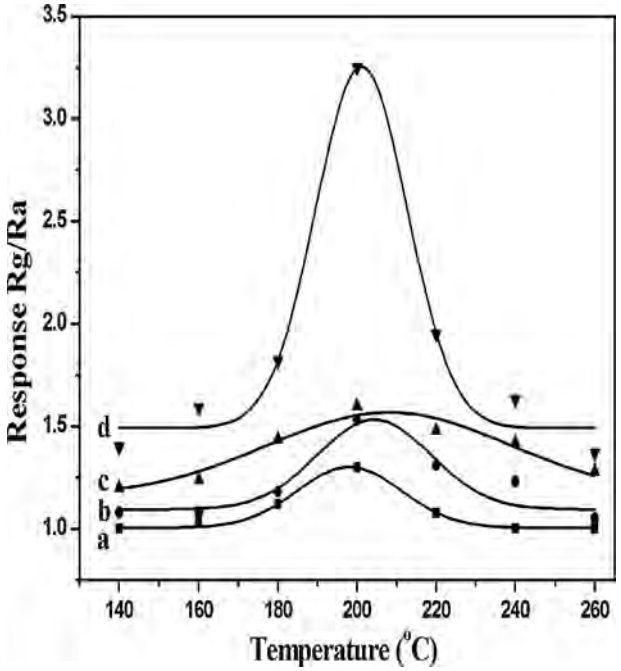

Fig. 8. Response values of sensors fabricated from NiO powders (a and b) and multilayer NiO products (c and d) to 100 ppm (a and c) and 500 ppm (b and d) formaldehyde at different temperatures.

and reached their maximum at 200 °C, and then decreased gradually with enhancing the temperature. This tendency was commonly observed for each sample. On the other hand, the response values of the same sensor were greatly enhanced by increasing the concentration of formaldehyde. Significantly, the multilayer NiO sensor exhibited higher sensing signal to formaldehyde than NiO powders sensor. This was own to the high surface-to-volume ratio which was formed by the nanofibers with nanogrooves. When the NiO sensors were exposed to air, oxygen molecules were adsorbed on the surface of NiO in the form of O^- and O^{2-} [13]. These oxygen species made the electrons transfer from the conduction band to the chemisorbed oxygen, resulting in a decrease in the conductance of the sensing layer. When the sensors were exposed to formaldehyde, as a reducing gas, formaldehyde reacted with adsorbed oxygen and released the electrons of the oxygen into the conduction band, leading to the decrease of the sensor resistance and thus generating electrical signals. High surface area can make NiO absorb more oxygen species, therefore the responses were enhanced.

4. Conclusion

In conclusion, multilayer NiO product was obtained by impregnating PLA nanofibrous webs with ethanol solution of nickel acetate and calcinating in air. The morphology from surface to center was nanogrooves inlaid film, hollow pores and honeycomb-like nanofibers with nanogrooves, successively. The calcined NiO products were characterized by TGA, DSC, and SEM techniques. Therefore, the formation mechanisms of the different morphologies were confirmed. XRD and FT-IR measurements demonstrated that the product was highly pure NiO with cubic structure. Formaldehyde was used to evaluate the sensitivity of the NiO products. In comparison with NiO powder, the mixed structural NiO exhibited a much higher sensing signal. These findings provide clues which lead us to believe that the NiO with new structure should represent a promising material for sensor research.

References

[1] J.R. Sohn, J.S. Han, Preparation and characterization of $NiO/CeO_2–ZrO_2/WO_3$ catalyst for acid catalysis, Journal of Industrial and Engineering Chemistry 11 (2005) 439–448.
[2] S.A. Needham, G.X. Wang, H.K. Liu, Synthesis of NiO nanotubes for use as negative electrodes in lithium ion batteries, Journal of Power Sources 159 (2006) 254–257.
[3] X.H. Xia, J.P. Tu, J. Zhang, X.L. Wang, W.K. Zhang, H. Huang, Electrochromic properties of porous NiO thin films prepared by a chemical bath deposition, Solar Energy Materials and Solar Cells 92 (2008) 628–633.
[4] R.H. Kodama, S.A. Makhlouf, A.E. Berkowitz, Finite size effects in antiferromagnetic NiO nanoparticles, Physical Review Letters 79 (1997) 1393–1396.
[5] H. Pang, Y. Shi, J. Du, Y. Ma, G. Li, J. Chen, J. Zhang, H. Zheng, B. Yuan, Porous nickel oxide microflowers synthesized by calcination of coordination microflowers and their applications as glutathione electrochemical sensor and supercapacitors, Electrochimica Acta 85 (2012) 256–262.
[6] G. Mattei, P. Mazzoldi, M.L. Post, D. Buso, M. Guglielmi, A. Martucci, Cookie-like Au/NiO nanoparticles with optical gas-sensing properties, Advanced Materials 19 (2007) 561–564.
[7] J.W. Lang, L.B. Kong, W.J. Wu, Y.C. Luo, L. Kang, Facile approach to prepare loose-packed NiO nano-flakes materials for supercapacitors, Chemical Communications (2008) 4213–4215.
[8] C. Yuan, X. Zhang, L. Su, B. Gao, L. Shen, Facile synthesis and self-assembly of hierarchical porous NiO nano/micro spherical superstructures for high performance supercapacitors, Journal of Materials Chemistry 19 (2009) 5772–5777.
[9] J. Hu, K. Zhu, L. Chen, H. Yang, Z. Li, A. Suchopar, R. Richards, Preparation and surface activity of single-crystalline NiO (1 1 1) nanosheets with hexagonal holes: a semiconductor nanospanner, Advanced Materials 20 (2008) 267–271.
[10] A. Aslani, V. Oroojpour, M. Fallahi, Sonochemical synthesis, size controlling and gas sensing properties of NiO nanoparticles, Applied Surface Science 257 (2011) 4056–4061.
[11] J. Li, R. Yan, B. Xiao, D.T. Liang, D.H. Lee, Preparation of nano-NiO particles and evaluation of their catalytic activity in pyrolyzing biomass components, Energy and Fuels 22 (2008) 16–23.
[12] J. Li, B. Xiao, L.J. Du, R. Yan, D.T. Liang, Preparation of nano-NiO particles and evaluation of their catalytic activity in pyrolyzing cellulose, Journal of Fuel Chemistry and Technology 36 (2008) 42–47.
[13] W. Zeng, B. Miao, L.Y. Lin, J.Y. Xie, Facile synthesis of NiO nanowires and their gas sensing performance, Transactions of Nonferrous Metals Society of China 22 (2012) s100–s104.
[14] W.K. Son, J.H. Youk, T.S. Lee, W.H. Park, The effects of solution properties and polyelectrolyte on electrospinning of ultrafine poly(ethylene oxide) fibers, Polymer 45 (2004) 2959–2966.
[15] X. Zhang, S. Xu, G. Han, Fabrication and photocatalytic activity of TiO_2 nanofiber membrane, Materials Letters 63 (2009) 1761–1763.
[16] N.G. Cho, H.S. Woo, J.H. Lee, I.D. Kim, Thin-walled NiO tubes functionalized with catalytic Pt for highly selective C_2H_5OH sensors using electrospun fibers as a sacrificial template, Chemical Communications 47 (2011) 11300–11302.
[17] H. Guan, C. Shao, S. Wen, B. Chen, J. Gong, X. Yang, Preparation and characterization of NiO nanofibres via an electrospinning technique, Inorganic Chemistry Communications 6 (2003) 1302–1303.
[18] J.A. Dirksen, K. Duval, T.A. Ring, NiO thin-film formaldehyde gas sensor, Sensors and Actuators B: Chemical 80 (2001) 106–115.
[19] C.Y. Lee, C.M. Chiang, Y.H. Wang, R.H. Ma, A self-heating gas sensor with integrated NiO thin-film for formaldehyde detection, Sensors and Actuators B: Chemical 122 (2007) 503–510.
[20] I. Castro-Hurtado, J. Herrán, G.G. Mandayo, E. Castaño, Studies of influence of structural properties and thickness of NiO thin films on formaldehyde detection, Thin Solid Films 520 (2011) 947–952.
[21] Y. Zheng, J. Wang, P. Yao, Formaldehyde sensing properties of electrospun NiO-doped SnO_2 nanofibers, Sensors and Actuators B: Chemical 156 (2011) 723–730.
[22] L. Liu, Y. Zhang, G. Wang, S. Li, L. Wang, Y. Han, X. Jiang, A. Wei, High toluene sensing properties of $NiO–SnO_2$ composite nanofiber sensors operating at 330 °C, Sensors and Actuators B: Chemical 160 (2011) 448–454.
[23] M. Liu, Z. Cheng, J. Yan, L. Qiang, X. Ru, F. Liu, D. Ding, J. Li, Preparation and characterization of TiO_2 nanofibers via using polylactic acid as template, Journal of Applied Polymer Science 128 (2013) 1095–1100.
[24] C.L. Shao, H.Y. Guan, S.B. Wen, B. Chen, D.X. Han, J. Gong, X.H. Yang, Y.C. Liu, Preparation and characterization of NiO nanofibers via an electrospinning technique, Chemical Journal of Chinese Universities 25 (2004) 1013–1015.
[25] R.C. Korošec, P. Bukovec, B. Pihlar, J.P. Gomilšek, The role of thermal analysis in optimization of the electrochromic effect of nickel oxide thin films, prepared by the sol–gel method. Part I, Thermochimica Acta 402 (2003) 57–67.
[26] X. Cao, Y. Xu, N. Wang, Facile synthesis of NiO nanoflowers and their electrocatalytic performance, Sensors and Actuators B: Chemical 153 (2011) 434–438.
[27] Y. Qiu, J. Yu, C. Tan, J. Yin, Preparation of honeycomb-like NiO with nanogrooves by using electrospun nanofibrous webs as templates, Materials Letters 63 (2009) 200–202.

Please cite this article in press as: M. Liu, et al., Preparation and characterization of multilayer NiO nano-products via electrospinning, Appl. Surf. Sci. (2013), http://dx.doi.org/10.1016/j.apsusc.2013.07.118